

1 **Assessment of Muscle Fatigue using Sonomyography: Muscle Thickness Change**
2 **Detected from Ultrasound Images**

3

4 Jun Shi ^{1,2} YP Zheng¹ X Chen¹ QH Huang¹

5 ¹ Department of Health Technology and Informatics, The Hong Kong Polytechnic
6 University, Hong Kong

7 ² School of Communication and Information Engineering, Shanghai University,
8 Shanghai, China

9

10 Running Title:

11 **Sonomyography Assessment for Muscle Fatigue**

12

13 Corresponding Author:

14 Yongping Zheng, PhD

15 Department of Health Technology and Informatics,

16 The Hong Kong Polytechnic University,

17 Hung Hom, Kowloon, Hong Kong SAR, P.R.China

18 Tel: 852-27667664

19 Fax: 852-23624365

20 Email: ypzheng@ieee.org

21

22 Submitted to: **Medical Engineering and Physics**

23 Date of Submission: **Jan 17 06**; 1st revision: **May 5 06**; 2nd revision: **Jun 28 06**

1 **Assessment of Muscle Fatigue using Sonomyography: Muscle Thickness Change**
2 **Detected from Ultrasound Images**

3
4 Jun Shi ^{1,2} YP Zheng¹ X Chen¹ QH Huang¹

5 ¹Department of Health Technology and Informatics, The Hong Kong Polytechnic
6 University, Hong Kong

7 ²School of Communication and Information Engineering, Shanghai University,
8 Shanghai, China

9
10 **Abstract:** Muscle fatigue is an exercise-induced reduction in maximal voluntary
11 muscle force. As the surface electromyography (SEMG) can be used to estimate the
12 features of neuromuscular activations associated with muscle contractions, it has been
13 widely employed as an objective tool to evaluate muscle fatigue. On the other hand,
14 ultrasound imaging can inherently provide the morphological information of
15 individual muscle, thus the architectural changes of muscles during fatigue can be
16 obtained. In this study, we demonstrated the feasibility of using the dimensional
17 change of muscles detected by ultrasound images, named as sonomyography (SMG),
18 to characterize the behavior of muscles when they were in fatigue. The SEMG signals
19 of the muscles were also recorded simultaneously and used for comparison. The right
20 biceps brachii muscles of 8 normal young male adult subjects were tested for 30s
21 under 80% of the maximal voluntary isometric contraction. The muscle fatigue was
22 indicated by the change of the root-mean-square (RMS) and median frequency (MDF)
23 of the SEMG signals. The results showed that the SEMG RMS had a linear increase

1 with time with a rate of 2.9 ± 1.9 %/s (mean \pm SD), while the MDF decreased
2 linearly with a rate of -0.60 ± 0.26 Hz/s. The muscle thickness, detected from the
3 ultrasound images, continuously increased during the muscle fatigue but with a
4 nonlinear increase with time, which was rapid during the initial 8.1 ± 2.1 s with a
5 mean deformation rate of 0.30 ± 0.19 %/s and then became slower with a rate of
6 0.067 ± 0.024 %/s up to 20 s after the contraction. The muscle deformation at 20 s
7 was 3.5 ± 1.6 %. The results demonstrated that the architectural change of muscles
8 detected using SMG could potentially provide complementary information for SEMG
9 for the muscle fatigue assessment.

10

11 **Key Words:** muscle fatigue, ultrasound, sonomyography, SMG,
12 electromyography, EMG, mechanomyography, MMG

13

14 **INTRODUCTION**

15 Muscle fatigue, which is an exercise-induced reduction in maximal voluntary
16 muscle force [1], frequently occurs in our daily life. It can be categorized into: 1)
17 central fatigue, defined as a decline of alertness, mental concentration, motivation,
18 and other psychological factors, and 2) peripheral fatigue defined as the changes in
19 physiological processes [1]. Many methods have been developed to evaluate muscle
20 fatigue, including oxygen uptake [2], heart rate [3], pH value of the muscle interstitial
21 fluid [4], muscle generated force [5], muscle stiffness [6], surface electromyography
22 (SEMG) [7][8], and invasive needle EMG [9], etc.

23 As muscle fatigue is an ongoing process during muscle activities rather than a

1 failure at a time point, it is important to monitor the temporal changes of the
2 physiological variables as the fatigue develops [8]. The SEMG signal, which contains
3 the features of the neuromuscular activation associated with the muscle contraction,
4 has been considered as an objective tool to evaluate muscle fatigue non-invasively.
5 The root-mean-square (RMS) and median frequency (MDF) of SEMG are frequently
6 used for the estimation of muscle fatigue. However, they are also sensitive to other
7 factors which may change during the muscle contraction [10]. Alternative signals with
8 the potential to tackle these challenges to SEMG are in demand and are being
9 explored in the related fields. For example, mechanomyography (MMG) [12]-[14],
10 which detects the sound or vibration generated by muscles during contraction, and
11 near-infrared spectroscopy [13] have been used for the assessment of muscle fatigue.

12 Since early 1990's, sonography has been used to measure the changes in muscle
13 thickness [15][16], muscle fiber pennation angle [17]-[20], muscle fascicle length
14 [15][17]-[20], and muscle cross-sectional area [17][21] during isometric and dynamic
15 contractions. As these architectural parameters have a close relationship with the
16 muscle functions [22], they can be potentially used to characterize muscle activities
17 during its contraction. Some researchers recently began to investigate the relationships
18 between the ultrasound parameters and the EMG activities in quasi-static [15][23][24]
19 and dynamic ways [25][26]. However, few studies have been conducted on muscles
20 fatigue using both ultrasound and EMG signals. Only most recently, two papers which
21 examined the muscle architecture with ultrasound during fatigue [25][26] were
22 reported.

23 The aim of this study was to investigate the feasibility of using the muscle

1 thickness change continuously extracted from the ultrasound images, named as
2 sonomyography (SMG) [16], to characterize the muscle fatigue. The ultrasound and
3 SEMG signals were collected simultaneously from the biceps brachii of 8 normal
4 young male adult subjects under an isometric contraction. The SEMG parameters
5 and the muscle deformation were calculated. The features of the muscle deformation
6 signal during muscle fatigue were described and its potential contributions to the
7 muscle fatigue evaluation were discussed.

8

9 **SUBJECTS AND METHODS**

10 Eight healthy male subjects participated in this study (age: 27 ± 3 years; height:
11 169 ± 3 cm; weight: 65 ± 5 kg). None of them had history of neuromuscular
12 disorders and each gave written informed consent prior to the experiment.

13 The subject was seated comfortably on the adjustable chair of a Cybex machine
14 (Cybex Norm Testing & Rehabilitation System, Cybex Norm Int. Inc., Ronkonkoma,
15 USA) with the trunk of the body fixed by a strap to the chair back to restrict the
16 posture change during the test. The forearm was placed and fixed on a forearm holder
17 and the hand gripped a vertical lever arm. The elbow was flexed at 90° with the upper
18 arm vertical and the forearm oriented horizontal. The axis of the lever arm was
19 mounted to be parallel with the rotational axis of the elbow joint. The hand was
20 maintained in the halfway between pronation and supination. The right arm was
21 chosen for measurements, which in all subjects was the dominant one.

22 After several warm-up contractions, three isometric maximal voluntary
23 contractions (MVC) were performed by each subject at the beginning of the

1 measurement. The subject was asked to produce the maximal isometric elbow flexion
2 at 90° as the MVC. The real time visual feedback of the torque value was displayed
3 on a computer screen. Each MVC lasted for approximately 3s with a rest interval of
4 60s between adjacent contractions. The MVC torque for each subject was defined as
5 the mean of the maximum values of the torque generated during the three
6 contractions.

7 When the experiment began, the subject was asked to perform an elbow flexion
8 against the lever arm to the 80% of his MVC [27] and maintained this value through
9 the visual feedback of the torque reading on the screen. The test was stopped when the
10 torque dropped to approximately 70% of the MVC. The data collection for the torque,
11 ultrasound image, and SEMG signal were started after the torque reached the 80%
12 MVC. To maintain the subject's concentration, constant encouragement was given
13 verbally during the contraction period. Usually, the endurance time did not exceed 30s
14 for all the subjects. Totally three repeated voluntary contractions were performed at
15 the same MVC level with a rest interval of at least 5 minutes [28][29] between
16 adjacent contractions.

17 A dynamometer (Cybex Norm Testing & Rehabilitation System, Cybex Norm Int.
18 Inc., Ronkonkoma, USA) was used to measure the elbow flexion torques. The torque
19 signals from the dynamometer were amplified by a custom-made amplifier and
20 digitized by a data acquisition card (NI PCI-6024E, National Instruments, Austin,
21 USA) installed in the PC, where they were synchronized with the ultrasound images
22 and SEMG signals. The experiment setup is shown in Fig. 1.

23 The ultrasound system used in this study was the same as that in a previous study

1 on the potential of SMG for prosthesis control [16]. The sonography of a
2 cross-sectional area of the biceps brachii was recorded using a portable B-mode
3 ultrasound scanner (180 Plus, Sonosite Inc., Washington, USA) with a 7.5 MHz / 38
4 mm linear probe (L38, Sonosite Inc., Washington, USA). The depth of the device was
5 46 mm. Under this setting, the corresponding pixel resolution was approximately 0.1
6 mm in both x and y directions. According to the measurements using phantoms, the
7 axial and lateral resolutions of the ultrasound image were 0.87 ± 0.13 mm, 0.92 ± 0.21
8 mm, respectively. The probe was fixed by a custom-made bracket and was
9 perpendicular to the skin surface of the biceps brachii region with its image plane
10 arranged vertically to the orientation of the biceps brachii muscle. The probe surface
11 had a distance from the skin surface to avoid any compression on the tissue during the
12 whole contraction period. Hence, the change of the muscle thickness was only
13 contributed by the behaviors related to the muscle fatigue. Ultrasound gel was used to
14 fill the gap between the probe and the skin to maintain a good coupling during the test.
15 The video output of B-mode ultrasound scanner was digitized by a video capture card
16 (NI PCI-1411, National Instruments, Austin, USA) with a sample rate of 8 Hz. The
17 images were saved frame by frame together with other signals for subsequent
18 analysis.

19 After cleaning the skin with alcohol, a pair of EMG bipolar Ag-AgCl electrodes
20 (Axon Systems, Inc., New York, USA) was placed between the transducer and the
21 elbow joint and near the ultrasound probe along the orientation of the biceps brachii
22 muscle. The distance between the two electrodes was approximately 20 mm. The
23 EMG reference electrode was placed on the proximal head of the ulna. The EMG

1 signal was amplified and filtered by a custom-made device with a gain of 10 and
2 bandwidth of 10-800Hz and then digitized by the A/D card (NI PCI-6024E National
3 Instruments, Austin, USA), which provided an additional gain of 10. The sample rate
4 for collecting EMG was 4 kHz.

5 The data acquisition was controlled by a custom-developed program for the
6 ultrasonic measurement of motion and elasticity (UMME) using Visual C++ 6.0
7 (Microsoft, Washington, USA) [16]. Multithread technology was applied in UMME
8 software to insure the synchronization among the ultrasound image, torque, and
9 SEMG. The ultrasound images were sampled frame by frame, each accompanied by
10 an SEMG epoch of 125 ms and a torque value.

11 All the ultrasound, SEMG and torque signals were processed off-line using the
12 UMME program and another program written in MATLAB (Version 6.5, MathWorks,
13 Inc., Massachusetts, USA). The ultrasound images were imported to the UMME
14 software and displayed frame by frame. A cross-correlation algorithm was used to
15 track the displacements of the interested tissue regions in the images. It has been
16 reported that the correlation tracking algorithm can work for images with low signal
17 noise ratio (SNR) and with complex structures of target and background [30], and is
18 particularly useful for the ultrasound images with complex speckles [16]. It requires a
19 reference image or template (containing the interested object) from an initial image
20 frame and looks for the most similar area to the reference image for estimating the
21 object position in the updated frame [30][31]. In this study, two rectangular blocks
22 were manually selected for the upper and lower boundaries of the cross-sectional
23 image of the biceps brachii in the first frame of the image sequences (Fig. 2a). The

1 images defined by these two blocks were regarded as two templates for the
2 subsequent automatic tracking. The echoes reflected from the muscle-humerus
3 interface were selected as the lower boundary of the elbow flexion muscles, which
4 were mainly the biceps brachii with a small portion of brachialis (Fig. 2). These
5 echoes were much easier to track in comparison with those from the fascia between
6 the biceps brachii and the brachialis. The centers of the upper and lower template
7 blocks were placed at the subcutaneous fat-muscle interface and the upper boundary
8 of the humerus, respectively (Fig. 2a). The sizes of the blocks were selected manually
9 to include enough features for a reliable tracking with a cross-correlation coefficient
10 larger than 0.9 between two conjunctive frames. This manual selection of the blocks
11 may slightly affect the value of the muscle thickness, but its effect on the deformation
12 measurement can be negligible. Figure 2a was taken at the moment when the torque
13 first reached 80% MVC and Fig. 2b at the moment when the torque started to
14 decrease to below that level. The image correlation tracking algorithm was
15 implemented in UMME software to track the movement of each selected block frame
16 by frame both in vertical and horizontal directions [16]. The equation used to
17 calculate the normalized two-dimensional cross-correlation is as follow:

$$18 \quad R(i, j) = \frac{\sum_{m=0}^{M-1} \sum_{n=0}^{N-1} [x(m, n) - \bar{X}][y(m, n) - \bar{Y}]}{\sqrt{\sum_{m=0}^{M-1} \sum_{n=0}^{N-1} [x(m, n) - \bar{X}]^2 \sum_{m=0}^{M-1} \sum_{n=0}^{N-1} [y(m+i, n+j) - \bar{Y}]^2}} \quad (1)$$

19 where $x(m, n)$ and $y(m+i, n+j)$ ($m=0, M$, and $n=0, N$) are the pixels of the
20 selected image blocks in two different frames. The image block $x(m, n)$ is regarded
21 as the template. The block represented by $y(m+i, n+j)$ shifts by i and j pixels in

1 the horizontal and vertical directions, respectively, in comparison with the template
2 represented by $x(m,n)$. \bar{X} and \bar{Y} represent the means of pixel density for the
3 image blocks $x(m,n)$ and $y(m+i,n+j)$, respectively, while $R(i,j)$ is the
4 cross-correlation coefficient between them. By changing i and j , the correlation
5 coefficients between the template in the first image and a group of image blocks in the
6 second image can be calculated. The best matched image block of the template can
7 then be located according to the peak value of the correlation coefficients. In this
8 study, the search range was set to be -10 to 10 pixels in the horizontal direction (i) and
9 -40 to 40 pixels in the vertical direction (j), respectively. After finishing the matching
10 for one frame, the template was automatically updated with the most similar image
11 blocks, which might shift from the position of the initial template. After the initial
12 template was manually selected, the above process would be automatically performed
13 for each subsequent image frame until the last one and the positions of matched image
14 blocks were recorded. It was demonstrated that the algorithm could achieve a
15 resolution of 0.1 mm for the displacement measurement for tracking the selected
16 image block, which was the same as the image pixel resolution.

17 The distance between the centers of the two image blocks was calculated for each
18 frame, which was defined as the muscle thickness at each moment. The percentage
19 deformation of the muscle was defined as:

$$20 \quad \rho = \frac{(d - d_0)}{d_0} \times 100\% \quad (2)$$

21 where d_0 is the initial muscle thickness at the moment when the subject first
22 contracted to 80% MVC, d is the muscle thickness measured at each frame.

1 The RMS of amplitude and MDF of the SEMG signals were calculated for each
2 epoch using the program written in MATLAB. The change rates of RMS and MDF as
3 functions of the muscle contraction time were further calculated using linear
4 regressions.

5

6 **RESULTS**

7 Figures 3a and 3b show the typical results of SEMG RMS and MDF for a trial on
8 one subject. In Fig. 3a, the y-axis was normalized by the first RMS value for each trial.
9 The results of other subjects showed similar trends. The increase of RMS and
10 decrease of MDF as a function of time during the muscle fatigue were consistent with
11 the results previously reported [7][32]-[34]. The changes of the SEMG parameters
12 confirmed that the investigated muscles had experienced fatigue during the
13 experiments. Figure 4a shows the increasing rate of SEMG RMS, and 4b the
14 decreasing rate of MDF of different subjects, with the error bars representing the
15 standard deviation (SD) of the three tests for each subject. The overall change rates of
16 SEMG RMS and MDF of the 8 subjects were 2.9 ± 1.9 %/s (mean \pm SD) and -0.60
17 ± 0.26 Hz/s, respectively.

18 Figure 3c shows the muscle deformation of the same subject as in Figs. 3a and 3b.
19 The muscle thickness increased obviously during the contraction, but in a complex
20 nonlinear manner. Figure 5 shows the muscle deformations of all the 8 subjects at 20 s
21 after the contraction. The overall mean deformation was $3.5 \pm 1.6\%$ at that moment.
22 During the first several seconds after the contraction, the muscle thickness increased
23 rapidly with a mean change rate of 0.30 ± 0.19 %/s for the 8 subjects (Fig. 6a). We

1 defined this rate as the initial muscle deformation rate. It lasted for 8.1 ± 2.1 s (Fig.
2 6c), and then the muscle thickness increased gradually with a smaller change rate of
3 0.067 ± 0.024 %/s (Fig. 6b) till the moment of the torque fluctuation, which
4 indicated that the subject could not maintain the assigned torque any more. We
5 defined this lower rate as the steady muscle deformation rate. The transition time
6 between the initial and steady muscle deformation rates was named as the critical time,
7 which was calculated as the cross point of the two linear trend lines as shown in Fig.
8 3c. From Fig. 3c, we can find that the deformation reached a peak at the time of
9 approximately 25s and then descended. This was because the subject could not
10 maintain the 80% MVC anymore and the torque tended to fluctuate. For all the
11 subjects, this phenomenon happened between 20 and 30 s of the experimental time.
12 Interestingly, this fluctuating torque was not reflected in the corresponding RMS or
13 MDF of the SEMG signals as shown in Figs. 3a and 3b.

14 The correlations between the muscle deformation and SMEG parameters were
15 also investigated. The R^2 values of the linear regressions were all smaller than 0.3,
16 indicating that no strong correlation could be observed between the muscle
17 deformation and the SEMG parameters during the fatigue of the muscle.

18

19 **DISCUSSION**

20 We described a method to simultaneously collect the SEMG signals and
21 ultrasound images of the biceps brachii muscle during an isometric contraction of the
22 80% MVC. From the SEMG signals, the RMS and MDF data were derived, while the
23 muscle deformation was obtained from the ultrasound images, i.e. sonomyography

1 (SMG). It was confirmed that the muscles experienced fatigue according to the
2 increase of RMS and the decrease of the MDF data [7][32]-[34]. It was also observed
3 that the muscle thickness increased rapidly during the first several seconds, then
4 increased gradually till the torque fluctuation, i.e. the subject could not maintain the
5 80% MVC. The transition of the muscle deformation rate might be explained as
6 follow_using the recruitment pattern and firing rate of the motor units during muscle
7 contraction.

8 In this study, the subject was asked to maintain a constant torque till he could not
9 persist and the joint angle remained constant during the test. The “size principle” [35]
10 suggested that more and more motor units might be recruited during the fatigue
11 process in order to compensate the inability of the activated muscle fibers and to
12 maintain their force generation [34]. According to the sliding filament theory of
13 muscle contraction [36], the newly recruited fibers could locally shorten to generate
14 enough force to maintain the torque. Consequently, the lateral dimension might
15 increase at some local regions. Furthermore, it has recently been reported that the
16 fascicle length significantly decreased and the pennation angle increased for the
17 gastrocnemius medialis muscle in vivo during the process of sustained isometric
18 contraction till fatigue [25]. The decreasing fascicle length and increasing pennation
19 angle were accounted for the creep of the corresponding tendon during the sustained
20 isometric contraction [25] and would result in the shortening of the muscle. According
21 to Swammerdam’s result [37] that the muscle volume kept constant during contraction
22 while the muscle shortening might cause the increase of muscle cross-sectional area
23 as well the muscle thickness [38]-[40]. Therefore, our finding of the increasing

1 muscle thickness during the sustained isometric contraction was consistent with the
2 result of this recent study [25], though the muscles studied were different. Further
3 studies should be followed to measure the creep of tendons and the dimensional
4 change of their corresponding muscles simultaneously seeking a better explanation for
5 the findings of the present study.

6 Interestingly, it was reported that the amplitude of the sound generated by the
7 muscle (mechanomyogram, MMG) showed a significant increase during the initial
8 phase of a sustained contraction and declined significantly when exhaustion was
9 approached [12]. Their results may correlate with our findings in this study. The
10 muscle sound is generated by the summation of the vibration of single motor unit
11 during contraction [41]. Further studies are required to systematically investigate the
12 mechanisms of the new findings observed in this study and the correlations among
13 different types of signals generated during the muscle fatigue.

14 We could not observe any indication of the torque fluctuation or the transition
15 phenomenon in the SEMG parameters (Fig. 3). The SEMG RMS and MDF linearly
16 increased and decreased, respectively, as time going during the whole measurement
17 even after the measured torque started to fluctuate. On the contrary, the results of
18 muscle deformation clearly indicated the torque fluctuation. This might reflect the fact
19 that the muscle deformation, similar to MMG, is a measure of actuation achieved
20 (mechanical output), while the SEMG is a measure of activation intended (electrical
21 input). As the muscle begins to fatigue, the neurons continue to fire at the same or
22 greater rate trying to activate the fibers to maintain the force output which results in
23 the continuous increase of the SEMG magnitude, but the fibers are unable to respond

1 causing the torque fluctuation. There is dissociation between the electrical and
2 mechanical activation of the muscle. Therefore, if we combine the information
3 provided by the muscle deformation and SEMG signals together, the muscle fatigue
4 can be potentially better characterized.

5 The subject number (n=8) is relatively small and only a specific group of subjects
6 (normal young male adults) were tested in this study. Since ultrasound imaging can
7 inherently provide the morphological information of individual muscles, it should
8 have potential to assess the fatigue of overlapped muscles. It has been reported that
9 the MMG parameters of biceps brachii and soleus muscles were significantly different
10 during the sustained isometric contraction [12]. Further investigations with diverse
11 and a larger number of subjects on different types of muscles are required to confirm
12 the potential applications of SMG for the fatigue analysis, particularly its capability of
13 differentiating neighboring deep muscles. It was noted that the variations of the
14 muscle deformation and SEMG parameters among the three repeated tests were
15 similar. For some subjects, the variations were relatively large. Therefore, it is
16 necessary to understand better in future studies what affects the extraction of the
17 parameters.

18 In this study, we used two rectangular blocks to automatically track the selected
19 upper and lower boundaries of the muscle for the sequence of real-time ultrasound
20 images using cross-correlation algorithm. The automatic correlation tracking was
21 performed for the image translating but not for rotation. It is possible that there is
22 rotational movement between the skin and the bone references during the muscle
23 contraction, particularly during the process of isometric or isotonic contractions. The

1 rotation of the muscle bundles was obvious during the process to reach the torque of
2 80% MVC, but not when a constant torque level was maintained. As described earlier,
3 all the data were collected after the torque reached 80% MVC, so the rotation should
4 have had minimal effect on the results. This could be confirmed by the high
5 correlation coefficient ($R > 0.9$) of the cross-correlation tracking for the skin reference
6 and the bone reference among the image frames collected during the fatigue process.
7 If a significant rotation happened for the tracking references, the correlation
8 coefficients would be reduced.

9 In conclusion, we demonstrated the feasibility of using the muscle deformation
10 signal extracted from real-time ultrasound images to characterize the muscle fatigue.
11 Both the SEMG and muscle deformation signals were used to monitor the muscle
12 fatigue of the biceps brachii under the isometric contraction. The results demonstrated
13 that the thickness of the biceps brachii increased first rapidly then gradually during the
14 process of fatigue with the transition moment at approximately 8 s after the
15 contraction reached 80% MVC. In addition, the torque fluctuation due to the failure to
16 maintain the required contraction level could be observed in the SMG signals, while
17 neither the transition phenomenon nor the torque fluctuation behavior could be
18 observed in the SEMG parameters (RMS and MDF), which changed linearly with the
19 time during the experiment period. The results suggest that the combination of the
20 muscle deformation signal and SEMG parameters may give more comprehensive
21 information for the fatigue assessment. The potential applications of the muscle
22 deformation monitoring of fatigue need to be further confirmed with more
23 experiments on subjects with different gender, age, and pathological conditions.

1

2 **ACKNOWLEDGEMENTS**

3

4 This work was partially supported by the Research Grants Council of Hong Kong
5 (PolyU 5245/03E), The Hong Kong Polytechnic University (A-PE63, G-U064,
6 G-YE22), and Shanghai Leading Academic Discipline Project (T0102).

7

8

9 **REFERENCES**

- 10 [1] Gandevia SC. Spinal and supraspinal factors in human muscle fatigue.
11 *Physiological Reviews*. 2001; 81(4): 1725-1789.
- 12 [2] Takaishi T, Ono T, Yasuda Y. Relationship between muscle fatigue and
13 oxygen-uptake during cycle ergometer exercise with different ramp slope
14 increments. *European Journal of Applied Physiology and Occupational*
15 *Physiology*. 1992; 65: 335-339.
- 16 [3] Laube W, Martin J, Tank J, Baeovski RM, Schubert E. Heart rate variability - An
17 indicator of the muscle fatigue after physical exercise. *Perfusion*. 1996; 9:
18 225-229.
- 19 [4] Stackhouse SK, Reisman DS, Binder-Macleod SA. Challenging the role of pH in
20 skeletal muscle fatigue. *Physical Therapy*. 2001; 12: 1897-1903.
- 21 [5] Cooper RG, Edwards RHT, Gibson H, Stokes MJ. Human-muscle
22 fatigue-frequency-dependence of excitation and force generation. *Journal of*
23 *Physiology*. 1988; 397: 585-599.

- 1 [6] Oka H. Estimation of muscle fatigue by using EMG and muscle stiffness.
2 Engineering in Medicine and Biology Society, 1996. Bridging Disciplines for
3 Biomedicine. Proceedings of the 18th Annual International Conference of the
4 IEEE. 1996; 4: 1449-1450.
- 5 [7] De Luca CJ. Myoelectrical manifestations of localized muscular fatigue in
6 humans. *Critical Review in Biomedical Engineering* 1984; 11: 251-279.
- 7 [8] Seghers J, Spaepen A. Muscle fatigue of the elbow flexor muscles during two
8 intermittent exercise protocols with equal mean muscle loading. *Clinical*
9 *Biomechanics*. 2004; 19: 24-30.
- 10 [9] Jensen BR, Pilegaard M, Sjogaard G. Motor unit recruitment and rate coding in
11 response to fatiguing shoulder abductions and subsequent recovery. *European*
12 *Journal of Applied Physiology*. 2000; 83: 190-199.
- 13 [10] MacIsaac DT, Parker PA, Englehart KB. A novel approach to localized muscle
14 fatigue assessment. Engineering in Medicine and Biology Society, 2003.
15 Proceedings of the 25th Annual International Conference of the IEEE. 2003; 3:
16 2487-2490.
- 17 [11] MacIsaac DT, Parker PA, Scott RN, Englehart K, Cechetto A. Influence of
18 dynamic factors on myoelectric parameters. *IEEE Engineering in Medicine and*
19 *Biology Magazine*. 2001; 20: 84-89.
- 20 [12] Kimura T, Hamada T, Watanabe T, Maeda A, Oya T, Moritani T.
21 Mechanomyographic responses in human biceps brachii and soleus during
22 sustained isometric contraction. *European Journal of Applied Physiology*. 2004;
23 92: 533-539.

- 1 [13] Yoshitake Y, Ue H, Miyazaki M, Moritani T. Assessment of lower-back muscle
2 fatigue using electromyography, mechanomyography, and near-infrared
3 spectroscopy. *European Journal of Applied Physiology*. 2001; 84: 174-179.
- 4 [14] Esposito F, Orizio C, Veicsteinas A. Electromyogram and mechanomyogram
5 changes in fresh and fatigued muscle during sustained contraction in men.
6 *European Journal of Applied Physiology*. 1998; 78: 494-501.
- 7 [15] Hodges PW, Pengel LHM, Herbert RD. Measurement of muscle contraction with
8 ultrasound imaging. *Muscle and Nerve*. 2003; 27: 682-692.
- 9 [16] Zheng YP, Chan MMF, Shi J, Chen X, Huang QH. Sonomyography: Monitoring
10 morphological changes of forearm muscles in actions with the feasibility for the
11 control of powered prosthesis. *Medical Engineering and Physics*. In print. 2006.
- 12 [17] Narici MV, Binzoni T, Hiltbrand E, Fasel J, Terrier F, Cerretelli P. In vivo human
13 gastrocnemius architecture with changing joint angle at rest and during graded
14 isometric contraction. *Journal of Physiology*. 1996, 496 (1): 287-297.
- 15 [18] Fukunaga T, Ichinose Y, Ito M, Kawakami Y, Fukashiro S. Determination of
16 fascicle length and pennation in a contracting human muscle in vivo. *Journal of*
17 *Applied Physiology*. 1997; 82: 354-358.
- 18 [19] Masamitsu Ito, Yasuo Kawakami, Yoshiho Ichinose. Nonisometric behavior of
19 fascicles during isometric contractions of a human muscle. *Journal of Applied*
20 *Physiology*. 1998; 85: 1230-1235.
- 21 [20] Maganaris CN, Baltzopoulos V and Sargeant AJ. Repeated contractions alter the
22 geometry of human skeletal muscle. *Journal of Applied Physiology*. 2002, 93:
23 2089-2094.

- 1 [21] Reeves ND, Maganaris CN, Narici MV. Ultrasonographic assessment of human
2 skeletal muscle size. *European Journal of Applied Physiology*. 2004, 91: 116-118.
- 3 [22] Liber RL. *Skeletal muscle structure, function, and plasticity*. Lippincott Williams
4 & Wilkins. 2002.
- 5 [23] Nordander C, Willner J, Hansson GA, Larsson B, Unge J, Granquist L and
6 Skerfving S. Influence of the subcutaneous fat layer, as measured by ultrasound,
7 skinfold calipers and BMI, on the EMG amplitude. *European Journal of Applied*
8 *Physiology*. 2003, 89: 514-519.
- 9 [24] McMeeken JM, Beith ID, Newham DJ. The relationship between EMG and
10 change in thickness of transversus abdominis. *Clinical Biomechanics*. 2004; 19:
11 337-342.
- 12 [25] Mademli L, Arampatzis A. Behaviour of the human gastrocnemius muscle
13 architecture during submaximal isometric fatigue. *European Journal of Applied*
14 *Physiology*. 2005; 94: 611-617.
- 15 [26] Mademli L, Arampatzis A, Walsh M. Effect of muscle fatigue on the compliance
16 of the gastrocnemius medialis tendon and aponeurosis. *Journal of Biomechanics*.
17 2006, 39: 426-434.
- 18 [27] Buonocore M, Opasich C, Casale R. Early development of EMG localized
19 muscle fatigue in hand muscles of patients with chronic heart failure. *Archives of*
20 *Physical Medicine and Rehabilitation*. 1998; 79: 41-45.
- 21 [28] Oberg T. Muscle Fatigue and Calibration of EMG Measurements. *J.*
22 *Electromyogr. Kinesiol*. 1996; 5: 239-243.
- 23 [29] Kleine BU, Schumann NP, Stegeman DF, Hans-Christoph Scholle. *Surface EMG*

- 1 mapping of the human trapezius muscle: the topography of monopolar and
2 bipolar surface EMG amplitude and spectrum parameters at varied forces and in
3 fatigue. *Clinical Neurophysiology*. 2000; 111: 686-693.
- 4 [30] Cao G, Jiang J, Chen J. An improved object tracking algorithm based on image
5 correlation. *IEEE International Symposium on Industrial Electronics*. 2004; 1:
6 598-601.
- 7 [31] Montera DA, Rogers SK, Ruck DW, and Oxley ME. Object tracking through
8 adaptive correlation. *Optical Engineering*. 1994; 33(1): 294-302.
- 9 [32] Petrofsky JS, Lind AR. Frequency analysis of the surface electromyogram during
10 sustained isometric conditions. *European Journal of Applied Physiology*. 1980;
11 43: 173-182.
- 12 [33] Petrofsky JS, Glaser RM, Philips CA, Lind AR, Williams C. Evaluation of the
13 amplitude and frequency components of the surface EMG as an index of muscle
14 fatigue. *Ergonomics*. 1982; 25: 213-223.
- 15 [34] Garland SJ, Enoka RM, Serrano LP, Robinson GA. Behaviour of motor units in
16 human biceps brachii during a submaximal fatiguing contraction. *Journal of*
17 *Applied Physiology*. 1994; 76: 2411-2419.
- 18 [35] Henneman E, Somjen G, Carpenter DO. Functional significance of cell size in
19 spinal motoneurons. *Journal of Neurophysiology*. 1965; 28: 560-580.
- 20 [36] Huxley AF. Muscle structure and theories of contraction. *Progress in Biophysics*
21 *and Molecular Biology*. 1957; 7: 255-318.
- 22 [37] Swammerdam J. *Bilia Naturae*. 1737. cited by T. Kardel, in *Journal of*
23 *Biomechanics*. 1990, 23: 953-965.

- 1 [38] Narici M. Human skeletal muscle architecture studied in vivo by non-invasive
2 imaging techniques: functional significance and applications. *Journal of*
3 *Electromyography and Kinesiology*. 1999, 9: 97-103.
- 4 [39] Nygren AT, Greitz D, Kaijser L. Changes in cross-sectional area in human
5 exercising and non-exercising skeletal muscles. *European Journal of Applied*
6 *Physiology*. 2000, 81: 210-213.
- 7 [40] Kardel T. Sstensen, Niels geometrical-theory of muscle-contraction (1667) - A
8 reappraisal. *Journal of Biomechanics*. 1990, 23: 953-965.
- 9 [41] Orizio C, Gobbo M, Diemont B, Esposito F, and Veicsteinas A. The surface
10 mechanomyogram as a tool to describe the influence of fatigue on biceps brachii
11 motor unit activation strategy. Historical basis and novel evidence. *European*
12 *Journal of Applied Physiology*. 2003, 90: 326-336.

1 **Figure Captions**

2 **Fig. 1** The experimental setup for the measurement of muscle fatigue with SMG and
3 SEMG. The area labeled with the small rectangle is magnified in the upper-left corner.

4

5 **Fig. 2** Motion tracking for the ultrasound images using the two dimensional
6 cross-correlation algorithm. (a) The image taken at the moment when the torque first
7 reached 80% MVC and (b) the image taken when the torque started to decrease below
8 80% MVC. Two rectangular blocks were selected on the upper and lower boundaries
9 of the cross-sectional image of the biceps brachii, respectively.

10

11 **Fig. 3** The changes of the SEMG parameters and the muscle deformation during the
12 process of fatigue for a typical trial of a subject. (a) The change of the SEMG RMS
13 normalized by the value of the first data point; (b) the change of SEMG MDF , (c) the
14 change of muscle deformation. Linear regression was used in (a) and (b) to obtain the
15 changing rates of SEMG RMS and MDF. For (c) the muscle deformation, two
16 deformation rates were defined, namely initial muscle deformation rate representing
17 the initial fast thickness change and steady muscle deformation rate representing the
18 slow thickness change after the initial phase. The cross point of the two linear
19 regression lines was defined as the critical time. The circled region indicates that the
20 subject could not maintain the assigned torque any more due to fatigue and the torque
21 value started to fluctuate.

22

23 **Fig. 4** The mean change rates of SEMG parameters of the 8 subjects calculated from

1 the results of 3 trials. (a) The mean change rate of the normalized RMS of different
2 subjects; (b) the mean change rate of MDF of different subjects. The overall means of
3 all the subjects' change rates of the normalized RMS and MDF were given by the last
4 bars in (a) and (b), respectively. The error bars of the individual results represent the
5 SD of the 3 trials. The errors bars of the overall means represent the SD of the 8
6 subjects.

7

8 **Fig. 5** The mean muscle deformation for the 8 individual subjects at 20 s after
9 contraction at 80% MVC, which was calculated from the 3 trials. Their error bars
10 indicate the SD of the 3 trials. The overall mean muscle deformation for the 8
11 subjects' was given by the last bar with its error bar representing the SD of the values
12 of the 8 subjects.

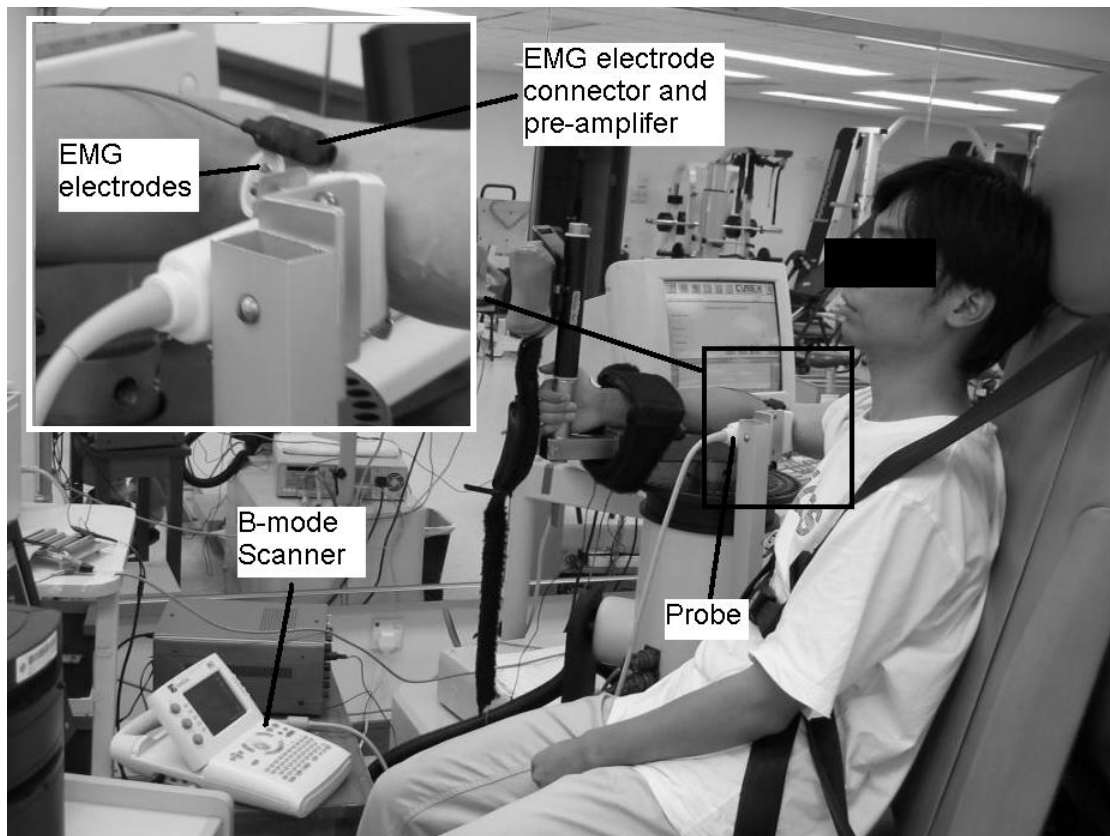
13

14 **Fig. 6** The mean parameters of SMG for the 8 subjects calculated from 3 trials. (a)
15 Initial muscle deformation rate; (b) steady muscle deformation rate; and (c) critical
16 time. The overall means of parameters calculated for the 8 subjects are shown in the
17 last bars in (a) to (c), respectively. The error bars of the individual results represent the
18 SD of the 3 trials, and the errors bars of the overall means represent the SD of the
19 values of the 8 subjects.

20

21

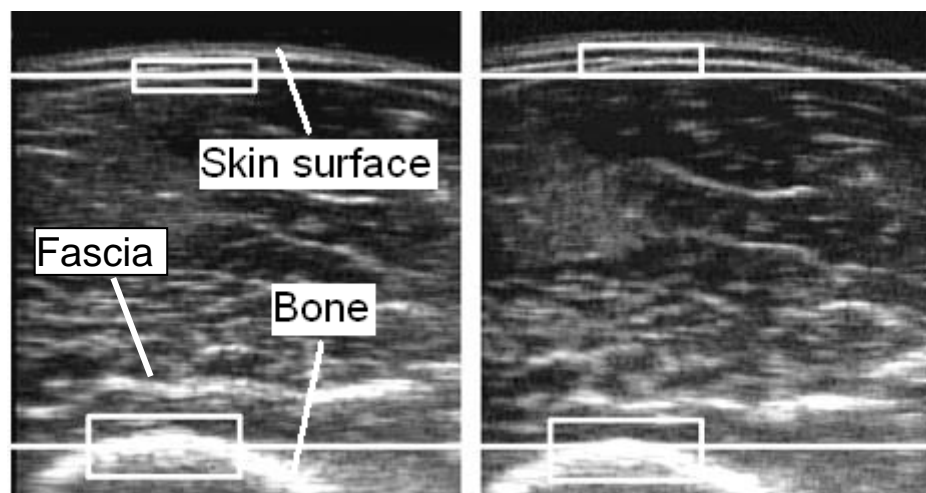
1 **Figures**



2

3 **Fig. 1**

4



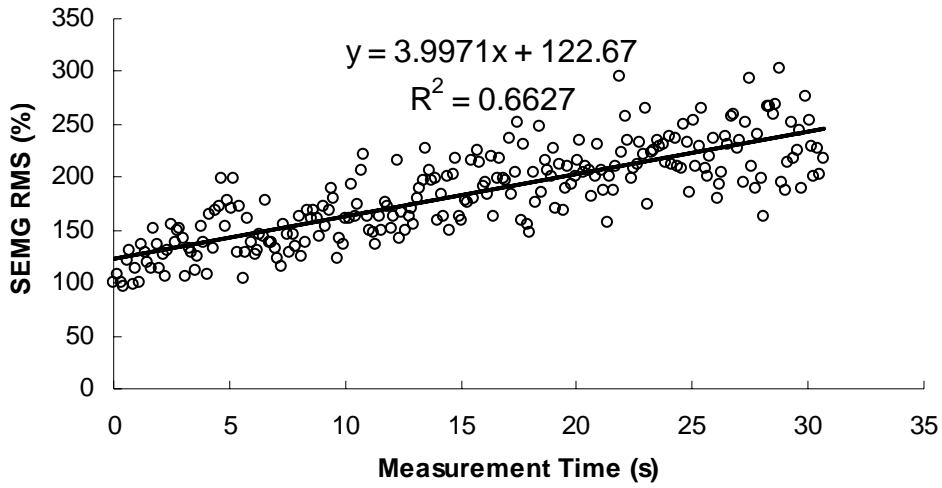
5

6 **(a)**

(b)

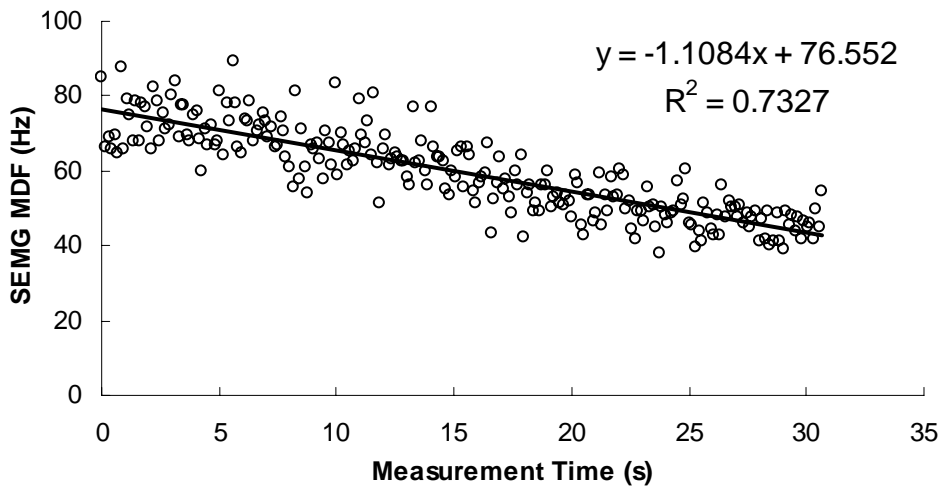
7 **Fig. 2**

8



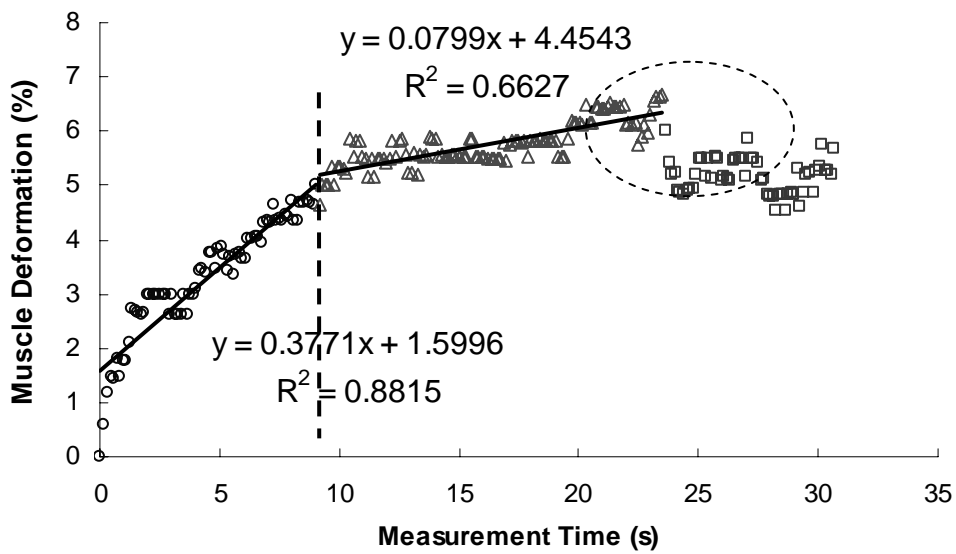
1

(a)



2

(b)

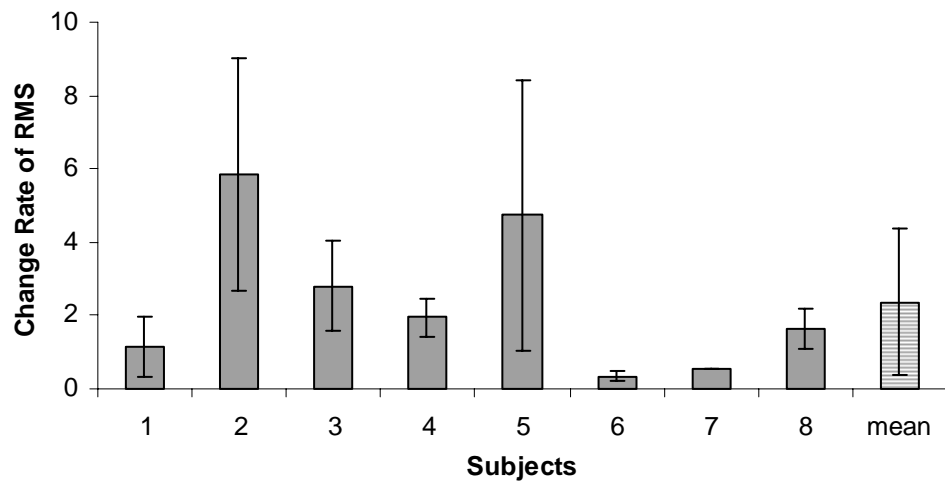


3

(c)

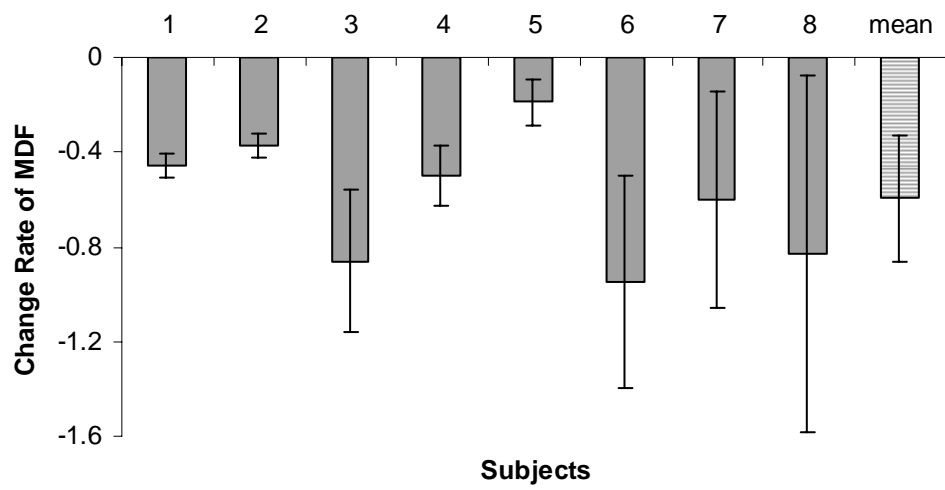
Fig. 3

5



1

2 (a)

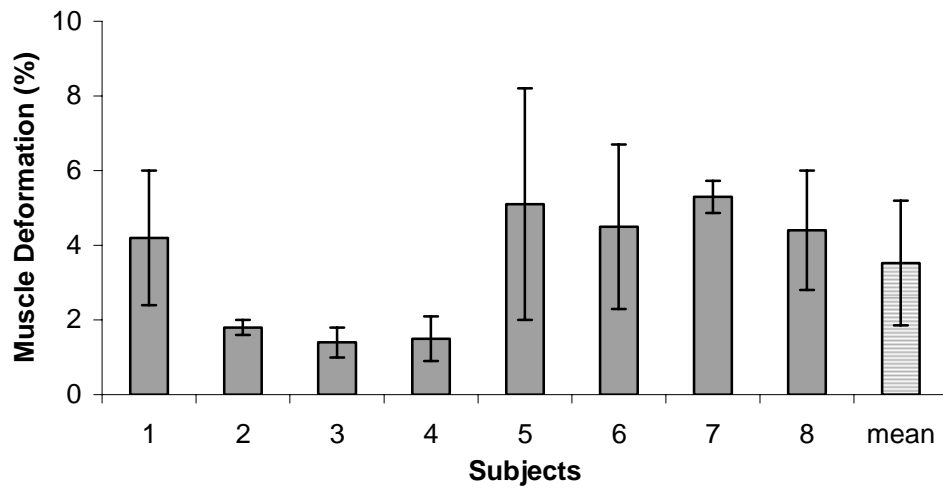


3

4 (b)

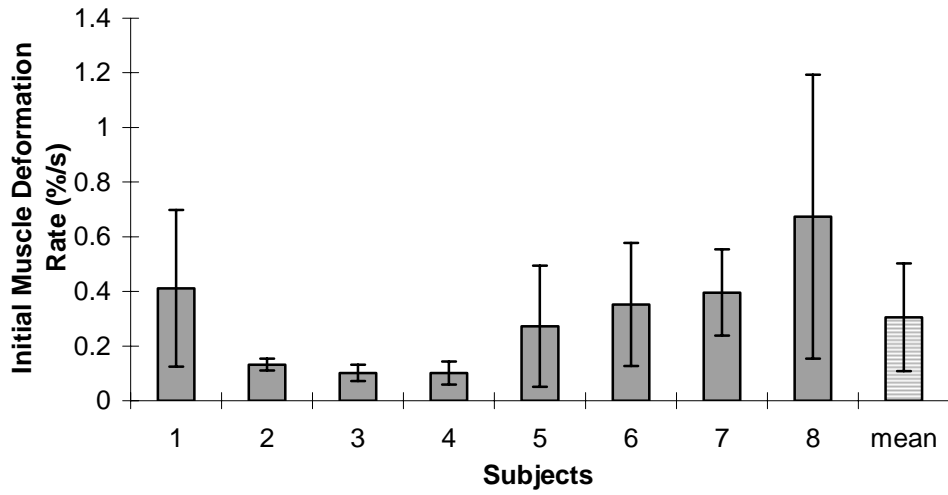
5 Fig. 4

6



1

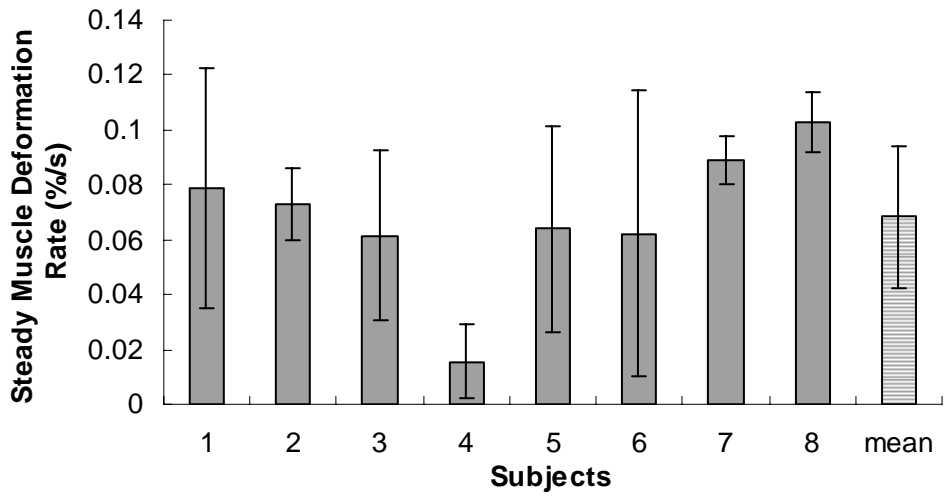
2 Fig. 5



1

(a)

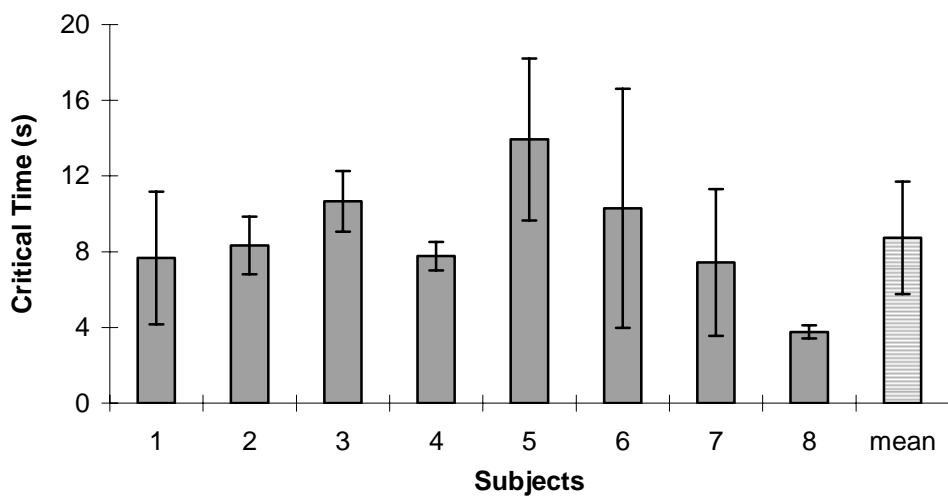
2



3

(b)

4



5

(c)

6 Fig. 6